

SULFIDES, STABLE ISOTOPES AND OTHER DIAGENETIC FEATURES OF THE MESOZOIC CARBONATE-MARL-SHALE SUCCESSION IN NORTHERN ETHIOPIA

Worash Getaneh

School of Earth Sciences, Addis Ababa University, PO Box 1176, Addis Ababa, Ethiopia. E-mail: worashgetaneh@gmail.com

ABSTRACT: This study investigates the carbonate-marl-shale succession (usually called Antalo Limestone and Agula Shale) in northern Ethiopia. The purpose of this study is to explain the diagenetic features, diagenetic environments and factors controlling them. The study is conducted by characterizing the whole rock carbon and oxygen isotopes, trace elements, mineral and textural features. Thirty samples were analyzed for carbon and oxygen isotopes, Sr and Mn; the latter two elements are chosen because of their sensitivity to diagenetic alterations. Moreover, 24 thin sections and 5 polished sections were investigated using petrographic and ore microscopes. The diagenetic features identified include sulfidation, micritization, silicification, cementation, neomorphism, pressure solution, vein development and hematitization. Oxidation rims around early diagenetic sulfides, development of clear spary calcite cement, and development dissolution features are common in the Agula Shale and lower part of Antalo Limestone. The $\delta^{13}\text{C}$ of the Antalo Limestone ranges from -0.23‰ to 2.22‰ PDB and $\delta^{18}\text{O}\text{‰}$ is between -7.42‰ and -3.16‰ PDB. In the Agula Shale $\delta^{13}\text{C}$ is between -3.25‰ and -0.12‰ and $\delta^{18}\text{O}$ ranges from -17.07‰ to -6.48‰ . The Mn/Sr ratio is higher for the Agula Shale (2.12) compared to that of the Antalo Limestone (0.35). The paleo-temperature estimation from oxygen isotope data suggested that the temperature experienced by rocks of the study area is between 56 and 26°C . These diagenetic and geochemical data suggest that the diagenetic environment varied from marine-phreatic to meteoric-phreatic environment. Furthermore, the diagenetic environment of Agula Shale is different from that of Antalo Limestone. The Agula Shale shows more influence of meteoric diagenetic fluid than Antalo Limestone does, which may be due to the early Cretaceous uplift in Eastern Africa. Neither textural (mainly abundance of framboidal pyrite and absence of open space filling sulfides) nor paleo-temperature data indicate any hydrothermal activity in the basin. Sulfides in the succession are thus the result of normal diagenetic and fossilization process in a reducing environment during sediment burial.

Key words/phrases: Carbonate, Diagenesis, East Africa, Stable Isotopes, Sulfide

INTRODUCTION

The systematic study of stable isotopes, trace elements, and diagenetic textures of sedimentary rocks is vital to understand many aspects of rocks and their history of formation (Dickson and Coleman, 1980; Allan and Matthews, 1982; Vincent et al., 2007; Aghae et al., 2014; Heidari and Shokri, 2015). Diagenetic environments, nature of diagenetic agents, geodynamic situation of depositional basins and subsequent alterations are some of the features studied using geochemical and textural data. Moreover, diagenetic fluids can be heated during deep burial of sediments accompanying substantial subsidence and subsequent rapid sedimentation. This situation leads to hydrothermal activities and formation of sedimentary ore deposits (called telethermal ore deposits) like the Mississippi Valley Type (MVT) Pb-Zn deposits (Sverjensky, 1984 and 1986;

Spangenberg et al., 1996). Isotopic and textural studies may indicate whether hydrothermal activities took place in the potential host rocks (Lindsay and Martin, 1999; Peace et al., 2003; Chen et al., 2014). The $\delta^{13}\text{C}$ and $\delta^{18}\text{O}$ isotope compositions of mineralized carbonates commonly show depleted values (Beaty and Landis, 1990; Stegen et al., 1990; Thompson and Arehart, 1990).

In northern Ethiopia, there is an extensive occurrence of a carbonate-marl-shale succession of upper Jurassic (Oxfordian-Kimmeridgian) age. The Antalo Limestone (up to 800m thick) and Agula Shale (up to 250m thick) are the two groups of the succession (Arkin et al., 1971; Beyth, 1972; Bosellinig et al., 1997). However, the lithological distinction between the two units is not significant except the limited occurrence of gypsiferous unit in the latter. A carbonate-marl-shale succession with occasional occurrence of

sandstone and arenaceous limestone constitute both units. The boundary between Agula Shale and Antalo Limestone is not clear and its presence is even doubtful based on which Bosellini et al. (1997) classified the two units as one "Super-sequence".

The geochemical and diagenetic studies on Antalo Limestone and Agula Shale, in addition to presenting new data, will contribute to the understanding of the above-mentioned geologic features and events of the Mesozoic era. Moreover, this study tests the hypothesis that the occurrence of sulfides (pyrrhotite, pyrite, sphalerite, and chalcopyrite) in the Agula shale indicates the presence of a low grade - high tonnage base metal deposit of MVT (Jelenc, 1966; Senbeto Chewaka and De Wit, 1981; Getaneh Assefa, 1985; Getaneh Assefa et al., 1993).

Therefore, this research intends to understand the difference and similarity of the Antalo Limestone and Agula Shale in terms of their depositional and diagenetic environments. It will also shed light on the role of the early Cretaceous uplift on the depositional and diagenetic pattern of the sedimentary units in the region. The geological and geochemical data will enable to constrain the mode of formation of the sulfides in the succession. The lack of diagenetic and stable isotopic study on the Mesozoic rocks of the study area makes this contribution original and relevant to the characterization of the Mesozoic era in Ethiopia and that of Eastern Africa as a whole.

GEOLOGIC SETUP OF THE STUDY AREA

The Mesozoic sedimentary basins of Ethiopia are the result of the breakup and rifting of Gondwanaland (Bosellini, 1992; Bosellini et al., 1997). The overall fragmentation and subsequent opening of the Atlantic Ocean resulted in the formation of fault bounded or half-graben type basins in Ethiopia. Such basins and sediments deposited therein are found in the central (Abay Gorge), northern (Mekele Outlier) and eastern/southeastern (Ogaden Basin) parts of the country (Fig.1).

The formation of the sedimentary successions in these basins is the result of a complete transgression-regression cycle in which the south west end of the Tethys Ocean transgressed onto the continental land mass beginning at the Lower Jurassic. This event deposited the lower clastic unit (called Adigrat Sandstone or the Lower Sandstone) during the Triassic, then the Limestone-Marl-Shale succession (Antalo Limestone and Agula shale) during the Jurassic (Oxfordian-

Kimmeridgian) and at the end another clastic unit (Ambaradam Sandstone or Upper Sandstone) during Early Cretaceous.

In northern Ethiopia, the exposure of Limestone-Marl-Shale succession covers the Mekele outlier (Fig.1). This outlier is a more or less circular exposure of Paleozoic-Mesozoic sedimentary rocks surrounded by low-grade metamorphic rocks of Precambrian age and volcanic rocks of Cenozoic age. The Precambrian rocks mark the base of the succession. The clastic succession (namely Enticho Sandstone and Edaga Arbi glacial with a thickness of up to 150m each) of Paleozoic time unconformably overlay the Precambrian rocks. The Mesozoic formations (Adigrat Sandstone, Antalo Limestone and Agula Shale) follow the Paleozoic sediments. The Ambaradam Sandstone marks the top of the Mesozoic succession. The latest formations in the area are the Cenozoic volcanic rocks (Beyth, 1972).

The Mekele basin is a gentle ramp structure showing a progressive deepening towards the east. It is part of a large basin covering the Arabo-Nubian geographic extent during the Mesozoic (Bosellini et al., 1995, 1997). This depression has been active sediment repository of the time when extensive Mesozoic sediments deposited and found exposed in the present day Ethiopia, Saudi Arabia, Yemen and India (Bosellini, 1986, 1992; Bosellini et al., 1995, 1997). Subsequent to the opening of the Red Sea and rifting during the Cenozoic, these sediments appear as patches distributed in different parts of Eastern/North Eastern Africa and Arabia.

The Antalo Limestone in the study area is divided into four subunits (Bosellini et al., 1997). These are designated as (from the bottom to the top) A1, A2, A3, and A4 (Fig.2). However, towards the eastern part of the basin (i.e., Shiket), distinctions among these groups becomes unclear and the whole formation becomes argillaceous limestone. A1 is found exposed in the western margin of the basin around the locality called Agbe. It is the basal near shore facies constituted by grainstones, wackstones and some marl layers. Its upper part contains coral-stromatoporoid layer. A2 is arenaceous limestone. A3 is a relatively deepwater facies made up of micritic limestone. Its upper part displays a coral-stromatoporoid rich layer. A4 is a marl-limestone intercalation whose basal unit is rich in cherty limestone. Agula Shale is an intercalation of Shale, Marl and Marly Limestone with occasional patches of gypsum. Both Antalo Lime-

stone and Agula Shale are strongly affected by Cenozoic age dolerite sills and dykes.

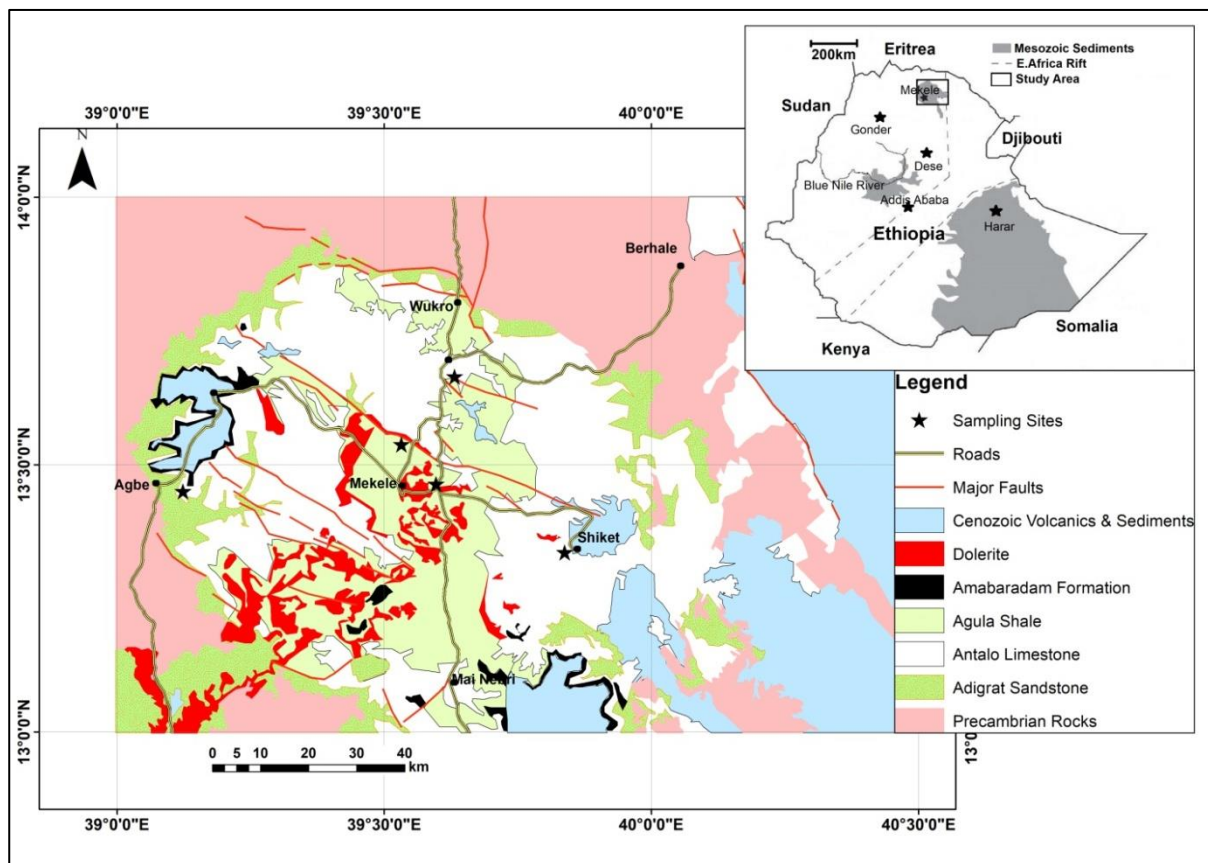


Figure 1. Geological Map of the Study area (Modified from Arkin et al., 1971)

METHODS AND MATERIALS

The Antalo Limestone and Agula Shale were sampled in different parts of the basin (Figs.1, 2). Thirty samples were collected and analyzed for whole rock carbon and oxygen isotopes, Sr and Mn. The choice of the elements Sr and Mn is based on the fact that they are sensitive to diagenetic alteration where Sr generally decreases with diagenetic stabilization while Mn shows degree of clastic input and redox conditions of the basin during deposition and diagenesis (Brand and Veizer, 1980, 1981). The mineralogical and textural features of the rocks and minerals were studied using twenty-four thin sections and five polished sections under transmitted and reflected light microscopy, respectively.

Laboratory procedures for carbon-13 and oxygen-18 isotope analysis has followed the classical method of McCrea (1950) in which carbonate powder reacts in vacuum with 100% phosphoric acid at 25°C. Isotopic ratios have been determined by a Finnigan MAT 250 mass spectrom-

eter at the University of Turin, Italy. Results are reported in $\delta\%$ relative to the PDB standard. Analytical uncertainty is $\pm 0.5\%$ for $\delta^{13}\text{C}$ and $\pm 0.1\%$ for $\delta^{18}\text{O}$. For Sr and Mn, powdered samples were dissolved using HNO_3 , HF and HClO_4 . The solution was analyzed using ICP-MS at the University of Cagliari, Italy. Accuracy is within 0.7% of the international standard materials used (GSR-6). The diagenetic environments and other characteristics of the rocks have been interpreted using diagenetic features, isotopic and trace element data.

RESULTS

Sulfide Minerals

The sulfide minerals identified are pyrite, pyrrhotite, and trace amount of chalcopyrite. Previous works (e.g., Getaneh Assefa et al., 1993) reported the occurrence of sphalerite but this research work did not identify it. Pyrite occurs as microcrystalline mosaics (sooty pyrite), spheroidal aggregates (framboids, Fig.3a), euhedral crystals

(Fig.3b) and subhedral grains ranging in size from very fine (<0.01mm) to coarse (>2mm) (Fig.3c).
 grained replacing the whole fragment of a fossil (Fig.3c).

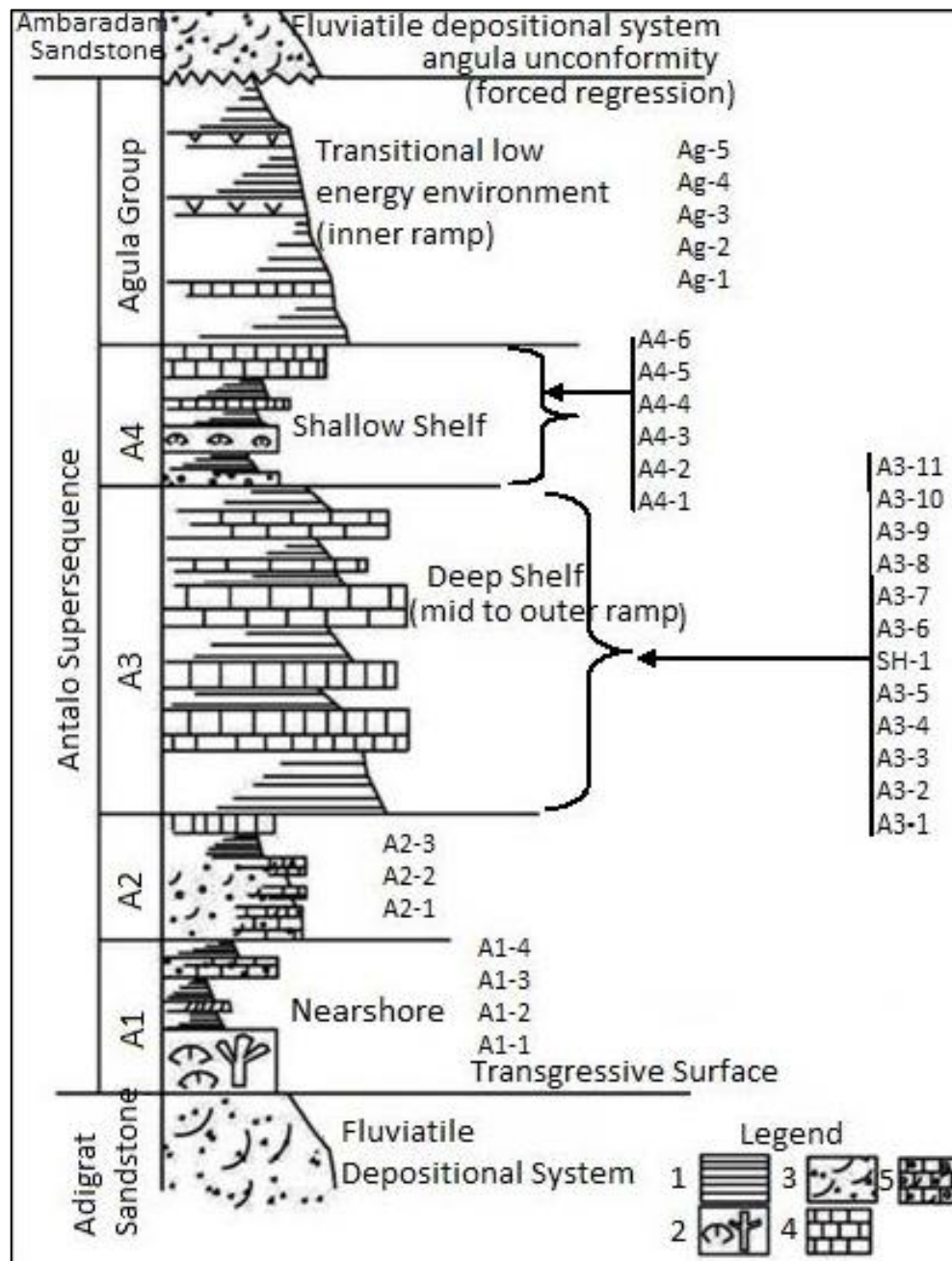


Figure 2. Composite Stratigraphy of the Mesozoic Succession in northern Ethiopia (not to scale, modified from Bosellini et al., 1995), and stratigraphic position of samples for this study (1-Marl, 2-Coral Stromatoporoid rich limestone, 3-Cross bedded Sandstone, 4-Limestone, 5-Cross bedded oolitic Limestone).

Some pyrite grains show replacement by chalcopyrite (Fig.3d). Pyrite occurs most often as fossil replacement (more commonly) and in the micritic matrix. The pyrite replaces both the fossil fragments and micrite indicating its early diagenetic nature. The fossil replacing pyrite destroyed the internal structure of fossils. Moreover, euhedral to anhedral pyrite replaces micrite matrix,

sparite (Fig.3e) and chert (Fig.3f) indicating a late diagenetic occurrence of some pyrite during burial diagenesis.

Micritization

Micritization has affected bioclasts (skeletal grains), ooids and pellets. It occurs as thin dark envelope around these grains (Fig.4a). In some

cases, micrite fills fossil molds and intragranular voids. Some of the micrites filling fossil chambers recrystallized into microsparite and sparite due

to neomorphism. Micritization destroyed partially to completely the internal structures of . bioclasts.

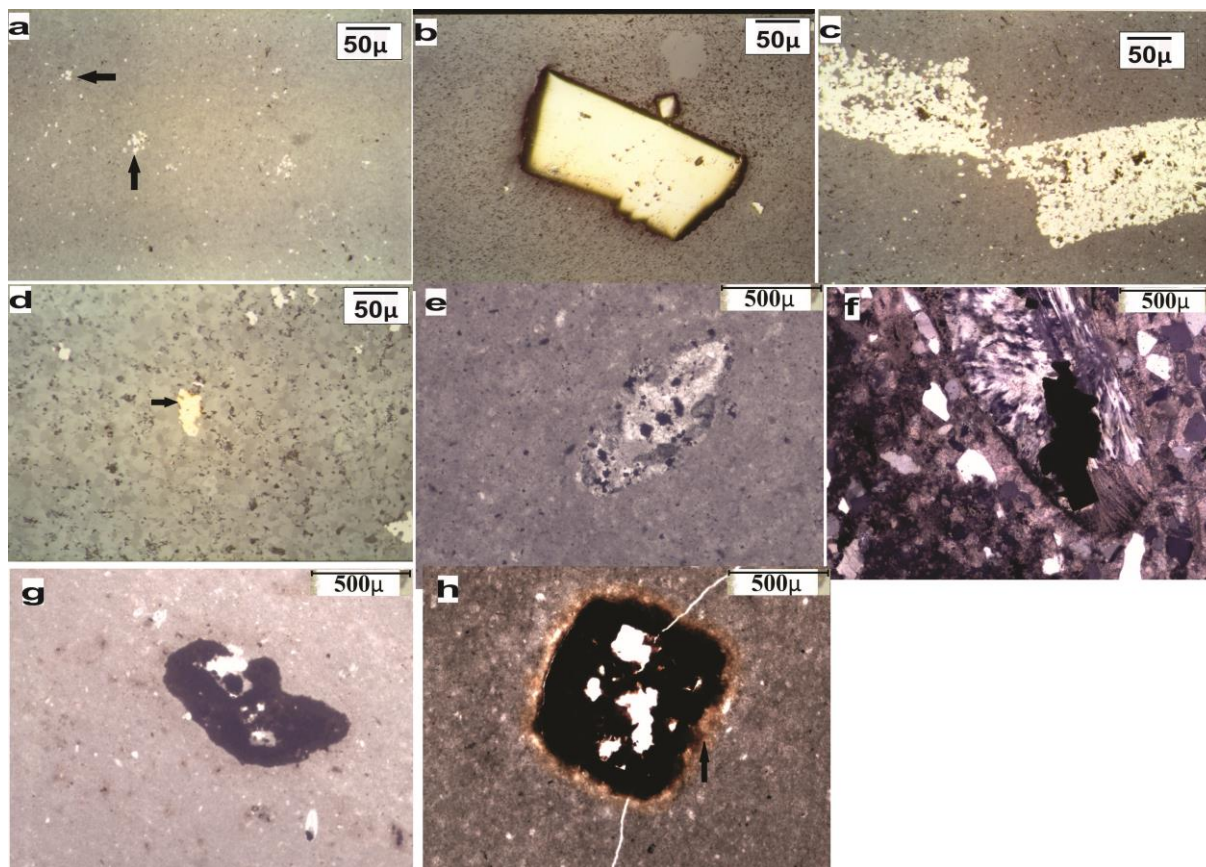


Figure 3. Different forms of sulfide occurrences (PPL=Plane Polarized Light; XPL=Crossed Polarized Light). (a) Framboidal Pyrite-polished section (PPL); (b) Euhedral pyrite replacing micrite-polished section (PPL); (c) Fossil fragments entirely replaced by pyrite-polished section (PPL); (d) Chalcopyrite replacing pyrite -polished section (PPL); (e) Anhedral pyrite replacing mold filling sparite-thin section (PPL) (f) Euhedral pyrite replacing chert-thin section (XPL); (g) Hematite grain (arrow)-thin section (PPL); (h) Sulfide oxidation into limonite/hematite -thin section (XPL)

Cementation

This event is less evident in micritic limestone that has neither bioclastic grains nor open spaces in which a cement can precipitate. This is dominantly evident in A3 and parts of A4, which are generally poor in fossil and other allochemical constituents. In some of the rarely observed bioclastic allochems, the mold filling material is sparite. This is more likely the result of neomorphism of the mould filling micrite. Stratigraphic units A1 and A2 display different degrees of cementation in which they display up to 60% sparite cement (Fig.4a,b), presence of blocky sparry calcite cement (Fig.4c,d), isopachous cement (Fig.4e), and syntaxial overgrowths (Fig.4f). The cement in all stratigraphic units has generally CaCO_3 composition except some limited pore and fenestrea filling chalcedonic cherts. The

mode of occurrence of the cement includes fossil mould filling drusy calcite, vug and channel filling, in intra- and inter-particle voids, fenestra filling and as fracture fillings.

Neomorphism

The dissolution and recrystallization of micrite, microsparite and sparite commonly appear in the analyzed thin sections. Neomorphism occurs both as recrystallization of lime mud (micrite) into microsparite - aggrading neomorphism (Fig.5a) in micritic limestone and as fillings of voids (mainly fossil shells) by sparite in grainstones and packstones. Such changes are expected to take place through dissolution and recrystallization of high magnesium calcite and aragonite lime mud in the presence of water during early to shallow burial diagenesis (Tucker

and Wright, 1990). Quartz grains decomposed into calcite along their margins (calcitization). The quartz grain veined by calcite (Fig.5b) suggests an advanced diagenetic stage where CaCO_3

saturated fluids acted upon previously existing allochemical grains in alkaline environment (Tucker and Wright, 1990).

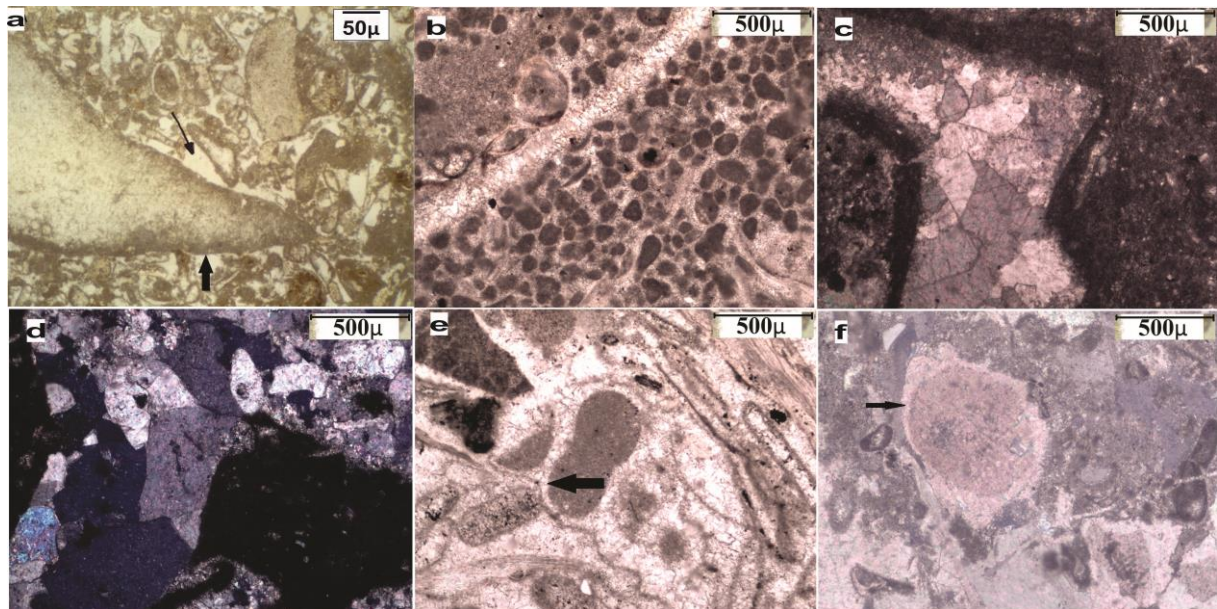


Figure 4. Cement formation (PPL=Plane Polarized Light; XPL=Crossed Polarized Light). (a) Clear sparite cement (small arrow) and micritization (big arrow) -thin section (PPL); (b) Sparite cement in pelloidal limestone -thin section (PPL); (c) Mold filling blocky calcite cement -thin section (PPL); (d) Intergranular blocky calcite cement -thin section (XPL); (e) Isopachous cement -thin section (PPL); (f) Syntaxial overgrowth around a crinoids fossil (arrow) -thin section (XPL)

Silicification

Authigenic subhedral to euhedral quartz crystals are abundant in most of the thin sections as pore-filling chalcedonic quartz and fossil replacing micro-quartz (chert nodules, Fig.5c). The silicification phenomenon developed well in the two coral-stromatoporoid layers (i.e. A1 and upper part of A3) where one can find megascopic nodules, layers and veinlets of chert.

The mode of occurrence of silicification is selective replacement of fossils (Fig.5c). When fossils are less abundant, the amount of silica in the form of chalcedony, chert nodules or authigenic quartz decreases proportionally. Silicification is also restricted to certain stratigraphic levels. The proximal facies (A1 and A2) are more silicified than other members are.

Dissolution and Porosity

The actual porosity of the rocks deduced from thin section observation is negligible. Carbonate cement occluded partially or completely all porosity types. Some porosity types available and visible under microscope are very limited in extent and reaches rarely 1-2% in some sections caused by post depositional dissolution, which

may be related to the action of meteoric waters; especially in the proximal facies of A1, A2 and Agula Shale. The available porosity types include mold, fenestral, vein, cavity, intergranular and intragranular. Calcite partially fills some veins central part of which remained empty. This would indicate lack of cementing material. The lower layer (A1), the arenaceous member (A2) and the last coral-stromatoporoid layer are more porous compared to other layers of the succession. Some intercalated layers of coquina, wackstone and packstone display better secondary porosity than the micritic limestone. The relatively porous layers within the sequence suggest dissolution by under saturated meteoric waters (Fig.5d).

Compaction

Compaction during diagenesis is a common phenomenon as sediments bury deeper leading to physical and chemical changes. Stylolites are indicators of such phenomenon (Tucker and Wright, 1990, Aghaei et al., 2014). Stylolites are rare occurrences in the study area except from some samples from layer A3 (Fig.5e). Moreover, the breakage of pyritized brachiopod fossil frag-

ment (Fig.3c) may be the result of differential compaction by sediment overburden.

Vein formation

Veins of different thickness and generation are common in the studied thin sections. Sparite and micro sparite calcite filled the veins (Fig.5f, g, h). Minerals do not fill some of the veins. Different stages of fracturing, dissolution and precipitation is evidenced by different generations of calcite-filled or empty veins that crosses previous ce-

ment, bioclastic grains, sparite (Fig.5g) and micrite filled fossil molds (lower left corner of Fig.4f) and pyrite grains (Fig.5f). Moreover, veins show breakage and displacement of a shortening nature (Fig.5h). Brittle fracturing in a shallow environment and formation of cracks and veins could be one of the results of uplift and the subsequent physical and chemical diagenetic changes in sedimentary rocks.

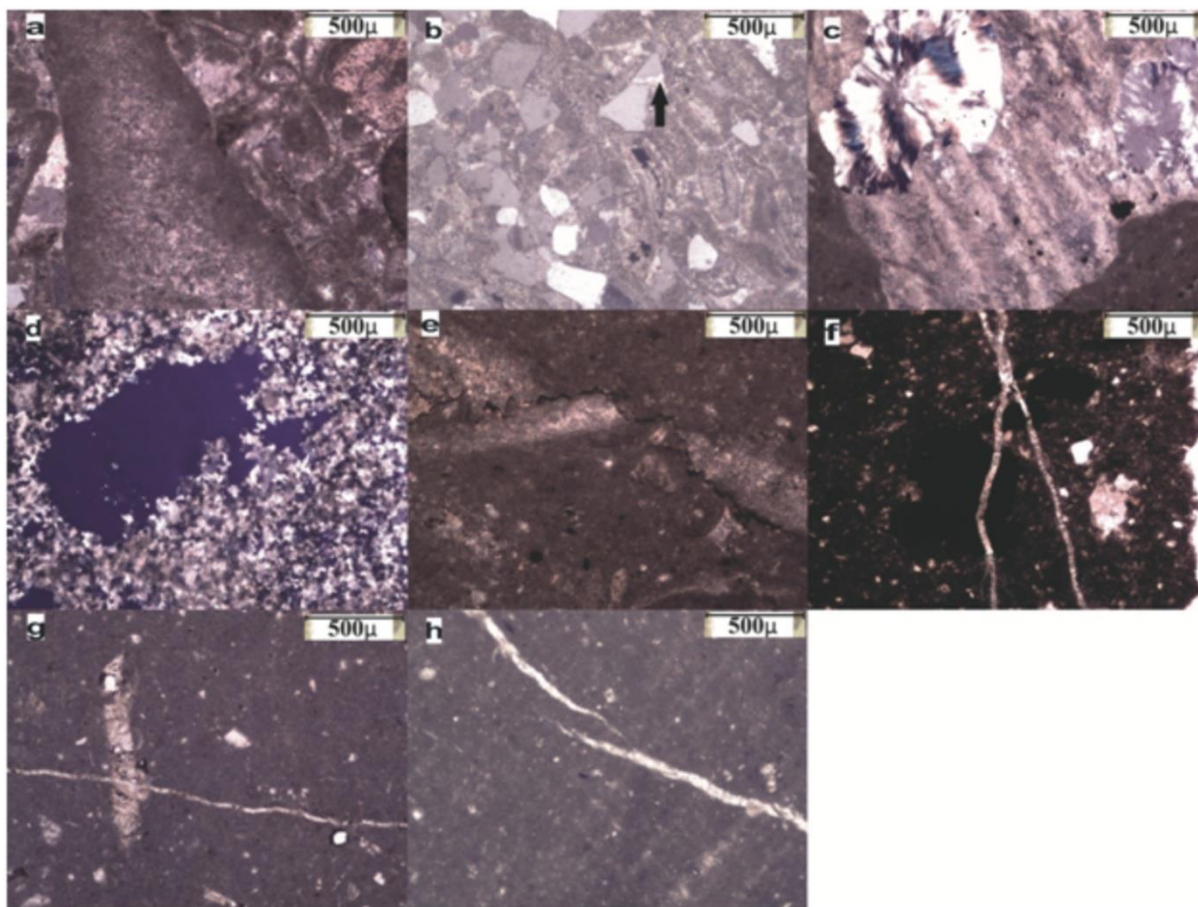


Figure 5. Some types of diagenetic features. (a) Partial neomorphism of a mold filling micrite-thin section (XPL); (b) detrital quartz grain changing into calcite (arrow) -thin section (XPL); (c) Fossil fragment altered into chert nodules-thin section (XPL); (d) Dissolution voids-thin section (XPL); (e) Stylolites-thin section (XPL); (f) Sparite veins crossing pyrite grains-thin section (XPL); (g) Vein crossing mold filling sparite-thin section (XPL); (h) Calcite filled broken veins-thin section (PPL)

Stable Isotopes and trace elements

Carbon Isotopes

The $\delta^{13}\text{C}$ values for the whole succession range from -3.25 to $+2.22\text{‰}$ averaging 0.50 . The data show that the samples fall into two distinct $\delta^{13}\text{C}$ groups with a mode of -1.34‰ for the light $\delta^{13}\text{C}$ (all samples from Agula Shale) and 0.95‰ for the heavy $\delta^{13}\text{C}$ group belonging to the Antalo Limestone (Table 1, Fig.6). The C-O isotope data clus-

ter into three groups (Fig.6). Field "I" represents Agbe section, which is the presumed paleo-coast of the Mesozoic sea in the study area. Field "II" is the rest of the Antalo Limestone (A2, A3 and A4) collected around Mekele. It is relatively towards the inner part of the basin. Field "III" is Agula Shale collected around Mekele and Agula localities (Fig.1).

The carbon isotopic data from the Antalo Limestone are positive except one sample from

Agbe section (A1), which may be localized effect of soil organic matter derived CO₂. The average values for each of the Antalo Limestone are all positive (A1=0.84; A2=0.71; A3=1.25; and

A4=0.52). It is worth noting that the deep marine facies A3 has the most positive carbon isotope value (2.22‰).

Table 1. Geochemical Composition of Antalo Limestone and Agula Shale (nd=not detected)

| Sample | δ ¹⁸ O‰ PDB | δ ¹³ C‰ PDB | Mn (ppm) | Sr (ppm) | Remark |
|--------|---------------------------|------------------------|----------|----------|---------------------------|
| AG-5 | -6.78 | -0.12 | 542.12 | 224.48 | Shaly Limestone (Agula) |
| AG-4 | -6.48 | -1.27 | 774.46 | 245.55 | Limestone (Agula) |
| AG-3 | -9.49 | -2.83 | 1006.80 | 353.71 | Shaly Limestone (Agula) |
| AG-2 | -7.35 | -0.31 | 232.34 | 251.14 | Shaly Limestone (Agula) |
| AG-1 | -17.07 | -3.25 | 387.23 | 250.87 | Shaly Limestone (Agula) |
| A4-6 | -4.43 | 0.60 | 77.45 | 169.80 | Limestone (Antalo) |
| A4-5 | -4.10 | 0.20 | 77.45 | 171.11 | Limestone(Antalo) |
| A4-4 | -5.48 | 0.08 | 77.45 | 180.89 | Limestone(Antalo) |
| A4-3 | -4.74 | 0.06 | 77.45 | 152.82 | Limestone(Antalo) |
| A4-2 | -4.90 | 0.92 | 309.78 | 270.15 | Marly Limestone(Antalo) |
| A4-1 | -3.85 | 1.23 | 232.34 | 158.75 | Marly Limestone(Antalo) |
| A3-11 | -3.16 | 0.46 | 232.34 | 246.46 | Limestone(Antalo) |
| A3-10 | -3.33 | 1.51 | 232.34 | 641.58 | Limestone(Antalo) |
| A3-9 | -6.32 | 2.22 | 77.34 | 505.54 | Limestone(Antalo) |
| A3-8 | -5.31 | 1.98 | 154.89 | 412.13 | Limestone(Antalo) |
| A3-7 | -7.16 | 1.05 | 154.89 | 509.56 | Marly Limestone(Antalo) |
| A3-6 | -5.83 | 0.26 | 154.89 | 409.8 | Marly Limestone(Antalo) |
| A3-5 | -5.71 | 1.77 | 77.45 | 364.24 | Limestone(Antalo) |
| A3-4 | -5.67 | 1.82 | 77.45 | 274.90 | Limestone(Antalo) |
| A3-3 | -3.99 | 0.96 | 154.89 | 619.78 | Limestone(Antalo) |
| A3-2 | -4.61 | 0.82 | 77.45 | 226.54 | Limestone(Antalo) |
| A3-1 | -4.86 | 0.87 | 77.45 | 261.15 | Limestone(Antalo) |
| SH-1 | -5.88 | 0.34 | 232.34 | 389.84 | Shaly Limestone(Antalo) |
| A2-3 | -4.90 | 1.08 | 232.34 | 261.49 | Sandy Limestone(Antalo) |
| A2-2 | -3.31 | 0.64 | 154.89 | 548.57 | Sandy Limestone(Antalo) |
| A2-1 | -4.18 | 0.40 | 464.68 | 314.95 | Sandy Limestone(Antalo) |
| A1-4 | -6.39 | -0.23 | 309.78 | 148.18 | Oolitic Limestone(Antalo) |
| A1-3 | -7.42 | 1.25 | nd | 223.73 | Oolitic Limestone(Antalo) |
| A1-2 | -6.41 | 1.03 | 77.45 | 317.86 | Limestone(Antalo) |
| A1-1 | -6.95 | 1.30 | 232.34 | 128.17 | Limestone(Antalo) |

Oxygen isotopes

The oxygen isotopic value varies from -3.16‰ to -17.1‰ with an average value of -5.87‰. However, highly depleted value of -17.1‰ can be considered as the result of localized conditions as it is far from the common value ranges seen in the sequence (-3.16‰ to -9.49‰). This sample is shaly limestone, silicified and is collected near a dolerite dyke. The average values for each of the group show that the Agula Shale has -7.53‰ (excluding the value of -17.1‰) or -9.43‰ considering -17.1‰, A4 -4.6‰, A3 -5.1‰, A2 -4.1‰, and A1 -6.8‰. The highly altered group is Agula followed by Agbe (-6.8‰). The average values are 2 to 3 times more depleted with respect to the expected values for marine carbonates of zero ±2‰ (Burdett et al., 1990; Prokoph et al., 2008).

Paleo-temperature of precipitation for minerals in the rock aggregate was estimated using the

following formula of Anderson and Arthur (1983).

$$T = 16.998 - 4.52(\delta_c^{18}O - \delta_w^{18}O) + 0.03 (\delta_c^{18}O - \delta_w^{18}O)^2$$

Where - T = the palaeo-temperature, δ_c¹⁸O = oxygen isotopic composition of the sample (PDB) and δ_w¹⁸O = oxygen isotopic composition of the seawater (SMOW) at the time of precipitation. The δ_w¹⁸O is taken to be -1.2‰ assuming ice free world (Shackleton and Kennet, 1975). The result (excluding -17‰) shows that temperature varies from 56°C to 26°C.

Trace elements

Manganese and strontium are selected for this study because of their significant sensitivity and hence their potential to show degree of diagenetic alteration (Brand and Veizer, 1980, 1981). As can be seen from table 2, strontium has higher concentration in A3 and Mn in Agula Shale. On

the other hand the minimum Mn/Sr ratio is in A3 while the ratio is higher in Agula Shale.

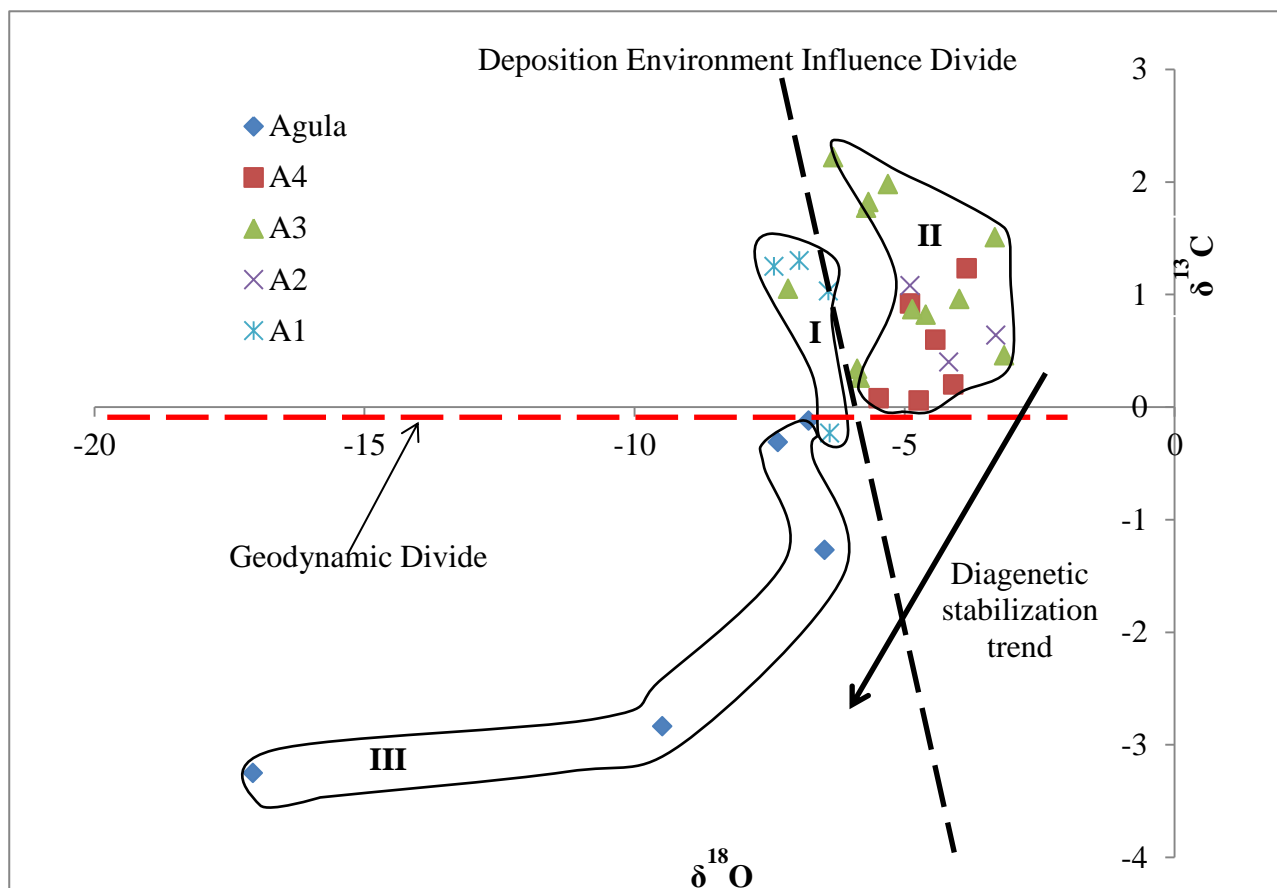


Figure 6. Oxygen versus carbon isotope values from the Carbonate-Marl-Shale succession of northern Ethiopia (note the distinctive field occupied by Agula group; Agbe section and the rest of the Antalo group)

Table 2. Average values of Sr, Mn and Mn/Sr for Antalo Limestone and Agula Shale

| Rock Units | Sr (ppm) | Mn (ppm) | Mn/Sr |
|-----------------|----------|----------|-------|
| Agula Shale | 269 | 589 | 2.12 |
| A4 | 184 | 142 | 0.77 |
| A3 | 407 | 134 | 0.33 |
| A2 | 375 | 284 | 0.76 |
| A1-Agbe section | 205 | 155 | 0.76 |

DISCUSSION

Diagenesis

The diagenetic environment and conditions of sediment diagenesis can be interpreted from mineralogical (e.g., transformation of aragonite or high magnesium calcite to low magnesium calcite), textural maturity (e.g., micrite to sparite, cementation, porosity) and isotopic (generally lighter isotopic signature) data (Brand and Veizer, 1980, 1981; Dickson and Coleman, 1980; Hudson, 1977; Joachimski, 1994; Morse and Mackenzie, 1990; Veizer, 1983). Accordingly, the data collected from Antalo Limestone and Agula

Shale are interpreted in terms of diagenetic environment as follows.

Cementation is well developed in A1, A2 and Agula Shale. The lower part of Antalo Limestone (i.e., A1 and A2) and Agula Shale display dominantly a clear sparite cement which is more likely precipitated in the meteoric-phreatic environment as suggested by clear appearance (Fig.4a,b), presence of blocky sparry calcite cement (Fig.4c,d), isopachous cement (Fig.4e), and syntaxial overgrowths (Fig.4f). Moreover, these units are relatively more silicified than the other members (i.e., A3 and A4) of Antalo Limestone. Mostly silica and iron for limestone replacement come

from the continent especially in shallow marine settings like ramps and platforms (Laschet, 1984). The fact that the depositional basin for the study area is a shallowly dipping ramp (Bosellini et al., 1997) suggests that the continental source is more evident than other intra-basinal sources. This implies also that the depositional and diagenetic environment for A1, A2 and Agula Shale is near to the continent. Differences in fossil distribution might also control the distribution of silicification. Fossils are easily silicified especially corals, brachiopods and bryozoans (Tucker, 1991).

Most of the sulfide minerals show complete to partial oxidation into limonite and hematite, especially in the lower part of Antalo Limestone and Agula Shale, which still indicates its exposure to oxidizing meteoric water. Dissolution and development of porosity is higher in the presumed proximal facies (Agula Shale, A1 and A2). The relatively porous layers within the sequence suggest the action of meteoric water during diagenesis because of lowering of sea level and subsequent penetration of under-saturated meteoric water into the carbonate subsystem leading to its dissolution and porosity development (Fig.5d). All these features are considered to be the result of precipitation from a range of possible diagenetic waters whose end members are connate and meteoric (Flügel, 2010).

The isotopic and trace element data are in agreement with the textural features in such a way that the rocks have been exposed to meteoric-phreatic to marine-phreatic diagenetic waters. The fact that A3 has the maximum carbon isotope value suggests that it underwent relatively less diagenetic alteration under the influence of vadose/phreatic meteoric water compared to other members of the sequence and hence preserved its marine carbon isotope signature. Carbonate rocks which undergone diagenesis in a closed or partially closed system with respect to carbon in a low water-rock ratio condition preserve their original marine carbon isotope (Brand and Veizer 1980, 1981). A shift in carbon isotope from the original marine signature, which is not far from zero (Burdett et al. 1990; Hoefs, 2009), requires a high water rock ratio in the presence of vadose meteoric water (Marshall, 1992). The absence of negative $\delta^{13}\text{C}$ values in Antalo Limestone does not rule out its exposure to fresh water. In addition to the consistent negative $\delta^{18}\text{O}$ values in the different stratigraphic levels, during temporary emergence continental plant life was not established and hence any subaerial fluids would not encounter sufficient source of light

carbon isotope (Brand and Veizer, 1981). In the Agula Shale, a distinct and consistent negative value (down to -3‰) of $\delta^{13}\text{C}$ is evident with an average value of -1.56‰. Even if the actual values are not far from the expected value ranges (+2 to -2‰, Veizer, 1983; Faure, 1986; Burdett et al., 1990) for marine carbonates, the consistent negative values unlike to other groups of the sequence shows that Agula Shale has a separate diagenetic history that was influenced by a phreatic-meteoric to phreatic marine diagenetic fluids.

When we see the $\delta^{18}\text{O}$, the values in Agula Shale and A1 are significantly lower than the other groups (Fig.6). On the graph, fields III and I have almost overlapping values of $\delta^{18}\text{O}$ less than the rest of the Antalo Limestone. They are separated from the rest of Antalo Limestone by an inclined vertical broken line which is designated here as "continental influence divide". This divide shows that Agula Shale and A1 of the Antalo Limestone show relative enrichment in light oxygen isotope. It is evident that Agula Shale (due to the uplift) and A1 from Agbe (due to its near shore position) have been in a more continental realm of diagenesis than the rest of Antalo Limestone. The graph also demonstrates that there is large scatter in $\delta^{18}\text{O}$ values than $\delta^{13}\text{C}$. The ranges of the data for $\delta^{18}\text{O}$ and $\delta^{13}\text{C}$ are 13.91 and 5.47 respectively. The corresponding standard deviation is 2.6060 for Oxygen and 1.2529 for Carbon. This scenario suggests that oxygen being more susceptible to change in the composition of fluids (Morse and Mackenzie, 1990), there was a relatively large fluctuation of oxygen isotope values because of the repeated and short-range sea level fluctuations. Sequence stratigraphic studies of the succession by Bosellini et al. (1995, 1997) suggested a series of sea level lowstands in the succession. Therefore, the oxygen isotope pattern is ascribable to the influence of phreatic-meteoric fluids.

The Antalo and Agula groups have the same lithological features. However, their diagenetic environment seems different. The possible explanation for this would be a geodynamic phenomenon that happened during their diagenetic history. It is related to the relative dropping of the sea level leading to the lowering of the ground water table leading to more influence of phreatic-meteoric water and hence shifting of the diagenetic environment from typical marine condition to phreatic meteoric conditions. Considering the tentative age of Agula Shale and the timing of the regression (Bosellini 1986 and 1992; Bosellini et al., 1997), the phenomenon overlaps

with the Eastern African uplift and hence this geodynamic event should have left its imprint by the O-C isotopic values of the Agula group. A horizontal broken line with a carbon value of a little less than zero depicts this phenomenon. This line is designated as the "Geodynamic Divide" to indicate the effect of the Early Cretaceous regional uplift that created a different diagenetic environment for the Agula group. The positive correlation between oxygen and carbon in Agula (0.80) is a further evidence of a meteoric water influence during diagenesis (Hudson, 1977; Dickson and Coleman, 1980; Joachimski, 1994). There is no correlation between O and C (-0.32) in A3 suggesting the absence of any covariation between C and O. This is a feature of marine limestone not affected by meteoric diagenesis (Hudson, 1977; Allan and Mathews, 1982; Jenkyns, 1996).

Finally, it is worth considering the whole succession together in light of the $\delta^{18}\text{O}$ and $\delta^{13}\text{C}$ relationship. The statistical correlation between isotopes of C and O for the whole succession is 0.67, which shows considerable co-variation between the two. Such type of covariance is typical of post depositional alteration under the influence of meteoric/phreatic fluids (Hudson, 1977; Joachimski, 1994). Moreover, a strong correlation of 0.83 between Fe and Mn in the whole Antalo Supersequence (Worash Getaneh and Valera, 2002) is an additional indication of a meteoric/phreatic diagenetic effect because these two elements increase together during meteoric alteration of carbonates (Brand and Veizer, 1980). The fact that the carbon isotope values are close to 1‰ cannot exclude this assertion, because carbon isotopes are less susceptible to diagenetic alteration compared to other components. Many authors (e.g., Jacobsen and Kaufman, 1999) confirmed that the sequence of susceptibility for water-rock interaction and alteration is $\text{O} > \text{Sr} > \text{C}$. Therefore, the positive values for carbon isotope do not exclude the phreatic/meteoric diagenetic environment for the succession.

The isotopic patterns discussed above are in consistent with the Sr and Mn/Sr values (Table 2). The maximum Sr value (407 ppm) and minimum Mn/Sr (0.35) are in stratigraphic level A3. Strontium decreases while Mn increases with increasing diagenetic alteration (Brand and Veizer, 1980; Veizer, 1983; Kaufman et al., 1993). Therefore, the least altered is A3 whereas Agula Shale is relatively the most altered as it shows the maximum Mn/Sr value of 2 and Mn content of 589ppm. A Mn/Sr value of less than 2 indicates

non-significant diagenetic alteration (Jacobson and Kaufman, 1999; Sial et al., 2001; Marquillas et al., 2007; Nagarajan et al., 2008; Kakizaki and Kano, 2009).

The Mn vs $\delta^{18}\text{O}$ isotope ratio plot (Fig.7) also indicates that the Agula group has undergone a diagenetic process under a relatively open and reducing diagenetic environment. Among samples of all groups, those of Agula group are far from the presumed marine carbonates field (R). Whereas samples falling towards "R" are diagenitized under closed system and more water-rock interaction condition because a partially closed system will give rise to limited external sources, buffering of the system by rock composition, and diagenetic fluids have relatively long residence time. This situation will create a chance to homogenize the composition of the different components of the diagenetic system towards the rock composition (Moss and Tucker, 1995).

Origin of Sulfides

It has been indicated (e.g., Berner, 1984; Carnfield and Raiswell, 1991; Flugel, 2010) that pyrite is one of the most important early diagenetic minerals in sedimentary rocks specially where there is abundant organic matter and hence reducing conditions were well established. Pyrite is thus indicator of anaerobic sulfidic diagenesis.

The pyrite in the study area is abundant in the Agula Shale and the presumed deep-water facies (A3). However, there is rare occurrence of pyrite in all parts of the succession. The distribution pattern is an indication of more reducing diagenetic condition in A3 and Agula Shale relative to the others. However, the cause for the prevailing redox condition in the two layers is different. In case of A3, it may be related to the deepening of the depositional basin while in case of Agula Shale it is due to the restricted nature of the lagoon environment in which localized pockets of reducing portions of the environment are present as a result of restricted water movement and hence stagnation of water.

Pyrite shows complete to partial oxidation into pseudomorphs of limonite/hematite, which occurs both as separate replacement grains (Fig.3g.) and ghost cover around the rims of pyrite crystals (Fig.3h). The oxidation is related to a change in the redox condition from negative to positive Eh, which most probably is because of uplift, which lowers the groundwater table. This brings the pyritized fossil in contact with oxygenated meteoric water. In case of the study area, two

probable causes of sub aerial exposure are possible. The first one is the number of minor regres-

sion events related to oscillation of the sea

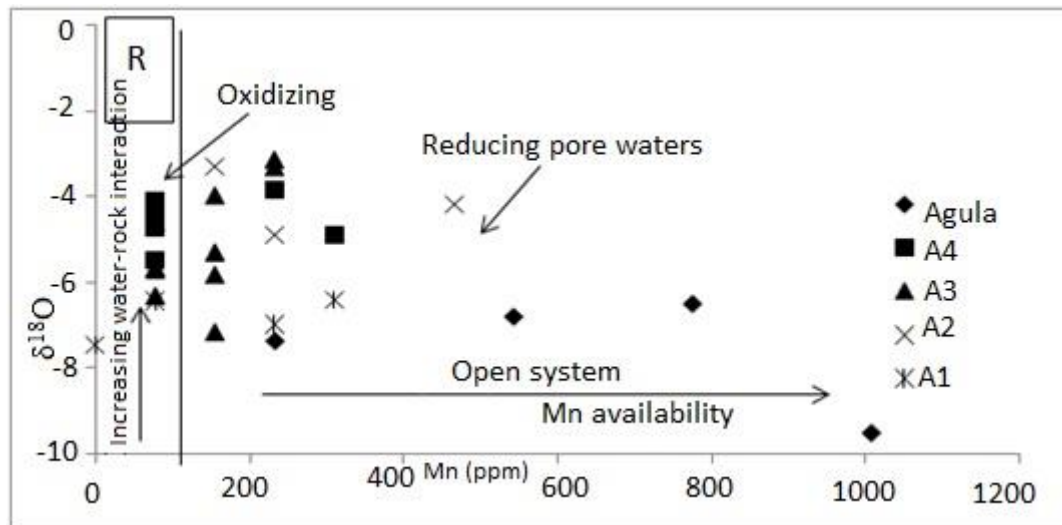


Figure 7. Scatter diagram of Mn vs. $\delta^{18}\text{O}$ for the study area (fields modified from Brand and Veizer 1980). "R" represents carbonates in equilibrium with present day seawater. Open System designates the field where no chemical differences between fossil and matrix/cement are evident

level during transgression, jerky subsidence. This is documented by the presence of a large number of discontinuity surfaces (hard grounds) in the whole succession. The second one is the final forced regression event during the early Cretaceous that caused the withdrawal of the Mesozoic sea from northern Ethiopia and finally East Africa (Bosellini et al., 1995, 1997).

The occurrence of Pyrrhotite and Chalcopyrite is restricted to samples collected near dolerite dyke and sill. Therefore, the formation of these sulfides is most likely due to a contact metamorphic effect where pyrite recrystallized in to pyrrhotite. Fine-grained chalcopyrite formed by replacing pyrite (Fig.3d) and in some cases the host rocks. The abundance of framboidal pyrites and pyritization of fossils are typical diagenetic features of sedimentary environments where sulfidation is a means of fossil preservation (Berner, 1984; Tucker, 1991).

Additional information is supplied by the paleo-temperature data calculated from oxygen isotope values. Temperature of precipitation could serve as source of information on the formation of minerals. In the case of sulfides occurrences in the study area, the possible process of formation is either a normal diagenetic process (as discussed above), or because of the action of hydrothermal fluids (in case MVT Pb-Zn mineralization took place). Temperatures of ore formation under hydrothermal process are usually

higher than temperature of normal diagenetic processes. Hence, data on temperature of precipitation of the minerals would shade light on whether there was action of heated water or not. Accordingly, the calculated temperature attained in the rocks (excluding -17‰) is between 56°C and 26°C. Using the above paleo-temperature, and considering that this is the maximum T expected in the calculation using the parameters without any correction, the maximum paleo-temperature attained by the rocks of the basin does not exceed 56°C. When we compare this range of temperature with world known deposits of carbonate hosted base metal deposits (e.g. Pin Point 80°C; Upper Mississippi Valley 125°C and South East Missouri 95-120°C; Sverjensky, 1986; Western Canada; 178-92°C; Hairuo and Mountjoy, 1994), it is too low. The worldwide survey on temperature of MVT deposits has shown that the mineralizing fluids have temperatures ranging from 60° to 250° with most temperatures falling between 100 and 150° (Gregg and Shelton, 2008). According to these authors, the rocks would have shown some features of hydrothermalism because mineralizing fluids can alter host rocks even far from the location of the actual ore deposits. Therefore, the preliminary paleo-temperature data indicates no sign of action of basinal brines. Moreover, the actual C and O isotope values in mineralized rocks of MVT deposits

are significantly very low (Sverjensky, 1986; Hairuo and Mountjoy, 1994; Leach et al., 2010). This is because of the common occurrence of organic matter (e.g., Sverjensky, 1984) in these deposits (applicable for carbon) and a relatively high temperature of deposition (for Oxygen) both of which are not typical of the study area (at least considering the C isotopic values).

Paragenetic sequence

Based on the diagenetic features described above, a tentative order of diagenetic/geologic events that took place in the Antalo Limestone and Agula Shale during the Jurassic-Cretaceous have been outlined. Marine, burial, uplift and meteoric stages are the four stages proposed for the study area.

- A) Marine Phreatic stage -Development of micrite and borings document this stage. The pyritization of fossils is part of this early stage of diagenesis.
- B) Meteoric Phreatic stage - the presence of blocky calcite, development of isopachous rim, and syntaxial overgrowth cements are indicative of diagenesis under meteoric phreatic condition (Tucker & Wright, 1990, Aghaei et al., 2014). However, the effect of meteoric phreatic diagenesis might have developed in some parts of the succession even

before this stage because of periodic sea-level lowstands as evidenced by previous studies (Bosellini et al., 1997). Therefore, some of the meteoric phreatic diagenetic features (mainly syntaxial and isopachous cement) mentioned above may date back to the marine phreatic diagenetic stages in the region.

- C) Burial stage - the presence of stylolites in layer A3 is possible indicator of burial diagenetic effect. Neomorphism of micrites and bioclastic grains including quartz characterizes this stage.
- D) Uplift - At this stage, lowering of groundwater table led to deeper penetration of meteoric water and migration of diagenetic environments from a marine phreatic to meteoric phreatic condition. The effects of this phenomenon should have possibly overlapped on previous temporary emergence of the land due to sea level fluctuations. The oxidation of sulfides and formation of limonite/hematite is the effect of the uplift followed by establishment of more oxidizing diagenetic conditions. Fracturing and formation of veins are part of this stage. Moreover, dissolution and formation of secondary porosity developed during this stage.

| | Marine Phreatic | Meteoric Phreatic | Burial | Uplift |
|--------------------------|-----------------|-------------------|-----------|--------|
| Micritization | ————— | | | |
| Pyritization | ————— | | ————— | |
| Silicification | ————— | ————— | | |
| Stylolitization | | | ————— | |
| Cementation (Isopachous) | | ————— | | |
| Cementation (Syntaxial) | - - - - - | ————— | | |
| Neomorphism | | ————— | ————— | |
| Fracturing | | | | ————— |
| Dissolution | | ————— | - - - - - | ————— |
| Hematitization | | | | ————— |

Figure 8. Sequence of events in the study area during late Jurassic to early Cretaceous

CONCLUSIONS

The carbonate-marl-shale succession in northern Ethiopia underwent a meteoric/phreatic to marine/phreatic diagenetic alteration. Diagenetic alteration is more evident in the Agula Shale than the Antalo Limestone. The latter preserved some features of a marine diagenesis effect especially with respect to its $\delta^{13}\text{C}$ values and textural features like micritization. On the other hand, the $\delta^{18}\text{O}$ values are low enough to indicate the composition of the marine carbonate rocks. Hence, the meteoric diagenetic fluids governed the oxygen isotope values of the whole succession and consequently we can say that the system was open with respect to $\delta^{18}\text{O}$. The Early Cretaceous uplift that caused the forced regression of the Mesozoic sea from present-day eastern/northeastern Africa may explain the difference in the diagenetic environment between Agula Shale and the Antalo Limestone.

Textural and stable isotopic data do not show any effect of hydrothermal activity in the study area. Therefore, the occurrence of sulfides is the result of common early diagenetic processes. Moreover, as evidenced by preferred pyritization of fossils, fossilization played important role in the formation of sulfides. Trace elements and isotopic data show that diagenesis took place in meteoric/phreatic and reducing diagenetic environment especially in the Agula Shale where sulfides are relatively abundant.

ACKNOWLEDGEMENT

The Author is grateful to the technical staff and geochemical laboratories of the University of Turin and University of Cagliari for the isotope and chemical analysis. School of Earth Sciences (Addis Ababa University) provided the researcher with financial support and field logistics.

REFERENCES

1. Aghaei, A., Mahboubi, A., Haramir, M., Nadjafi, M., and Chakrapani, G. J. (2014). Carbonate Diagenesis of the Upper Jurassic Successions in the West of Binalud - Eastern Alborz (NE Iran). *Journal Geological Society of India* 83, 311-328
2. Allan, J. R., and Matthews, R. K. (1982). Isotope signatures associated with early meteoric diagenesis. *Sedimentology* 29(6), 797-817
3. Anderson, T. F., and Arthur, M. A. (1983). Stable isotopes of oxygen and carbon and their application to sedimentologic and paleoenvironmental problems. In: Arthur M.A. (ed.), *Stable isotopes in sedimentary geology*. SEPM Short Course 10, pp.1-151
4. Arkin, Y., Beyth, M., Dow, D. B., Levitte, D., Temesgen Haile, and Tsegaye Hailu (1971). Geological map of Mekele Sheet area ND 37-11, Tigre Province. Geological Survey of Ethiopia, Addis Ababa
5. Beaty, D. W., and Landis, G. P. (1990). Gilman district: Part IV. Stable isotope geochemistry. *Economic Geology Monograph* 7, 228-245
6. Berner, R. A. (1984). Sedimentary pyrite formation: an update. *Geochim Cosmochim Acta* 48, 605-615
7. Beyth, M. (1972). Paleozoic-Mesozoic Sedimentary Basins of Mekele Outlier. Northern Ethiopia. *Association of American Petroleum Geologists Bulletin* 56, 2426-2439
8. Bosellini, A. (1986). East African continental margins. *Geology* 14, 76-78
9. Bosellini, A. (1992). The continental margins of Somalia. Structural evolution and sequence stratigraphy. *AAPG Memoir* 53, 185-205
10. Bosellini, A., Russo, A., Fantozzi, P. L., Getaneh Assefa, and Solomon Tadesse (1997). The Mesozoic succession of the Mekele Outlier (Tigre Province, Ethiopia). *Memorie Scienze Geologiche* 49, 95-116
11. Bosellini, A., Russo, A., and Getaneh Assefa (1995). Il Calcare di Antalo nella regione di Macallé (Tigrai, Etiopia Settentrionale). *Rend Fis Acc Lincei s.9, v.6*, 253-267
12. Brand, V., and Veizer, J. (1980). Chemical diagenesis of multicomponent system - 1: Trace elements. *Journal of Sedimentary Petrology*, 50, 1219-1250
13. Brand, V., and Veizer, J. (1981). Chemical diagenesis of multicomponent system - 2: Stable isotopes. *Journal of Sedimentary Petrology*, 51, 987-997
14. Burdett, J. W., Grotzinger, J. P., and Arthur, M. A. (1990). Did major changes in stable isotope compositions of seawater occur? *Geology* 18, 227-230
15. Chen, H., Xie, X., Mao, K., and Huang, J. (2014). Carbon and oxygen isotopes suggesting deep-water basin deposition associated with hydrothermal events (Shangsi section, northwest Sichuan basin-South China). *Chi-*

- nese Journal of Geochemistry (2014)33, 077-085
16. Dickson, J. A. D., and Coleman, M. L. (1980). Changes in Carbon and Oxygen isotopic composition during limestone diagenesis. *Sedimentology* 27, 107-118
 17. Faure, G. (1986). *Principles of isotope geology*. 2nd edn. Wiley, New York, 589pp
 18. Flugel, F. (2010). *Microfacies of carbonate rocks—analysis, interpretation and application*. Springer, Berlin, 984pp
 19. Getaneh Assefa (1985). The mineral industry of Ethiopia: present condition and future prospects. *Journal of African Earth Sciences* 3(3), 331-345
 20. Getaneh Assefa, Pretti, S., and Valera, R. (1993). An outline of the metallogenic history of Ethiopia. In: Abbate E., Sagri M., Sassi F P (Eds.), *Geology and mineral resources of Somalia and surrounding regions*. Ist. Agron. Oltramare, Firenze, Relaz. E Monogr. 113:569-578
 21. Gregg, J. M., and Shelton, K. L. (2008). Epigenetic dolomitization and Mississippi Valley type mineralization in Cambro-Ordovician carbonates of North America. AAPG Annual Convention, San Antonio, TX
 22. Hairuo, Q., and Mountjoy, E. W. (1994). Formation of coarsely crystalline hydrothermal dolomite reservoirs in the Presqu'île Barrier, Western Canada sedimentary basin. *AAPG Bulletin* 78, 55-78
 23. Heidari, A., and Shokri, N. (2015). Application of petrography, major and trace elements, carbon and oxygen isotope geochemistry to reconstruction of diagenesis of carbonate rocks of the Sanganeh Formation (Lower Cretaceous), East Kopet-Dagh Basin, NE Iran. *Arab J Geosci* (2015) 8:4949-4967
 24. Hoefs, J. (2009). *Stable Isotope Geochemistry*. 6th Edn. Springer, Berlin, 285pp
 25. Hudson, J. D. (1977). Stable isotopes and limestone lithification. *Geol. Soc. AM. Bull.* 133, pp. 637-660
 26. Jacobson, S. B., and Kaufman, A. J. (1999). The Sr, C and O isotopic evolution of Neoproterozoic seawater. *Chemical Geology* 191, 37-57
 27. Jelenc, D. A. (1966). *Mineral occurrences of Ethiopia*. Imperial Ethiopian Government, Ministry of Mines, Addis Ababa
 28. Jenkyns, H. C. (1996). Relative sea-level change and carbon isotope: data from the upper Jurassic (oxfordian) of central and southern Europe. *Terra Nova* 8, 75-85
 29. Joachimski, M. M. (1994). Subaerial exposure and deposition of shallowing upward sequences: evidence from stable isotopes of Purbeckian peritidal carbonates (basal Cretaceous), Swiss and French Jura Mountains. *Sedimentology* 41, 805-824
 30. Kaufman, A. J., Jacobsen, S. B., and Knoll, A. H. (1993). The vendian record of Sr and C isotopic variations in seawater: implications for tectonics and paleoclimate. *Earth Planetary Science Letters* 120, 409-430
 31. Laschet, C. (1984). On the origin of cherts. *Facies* 10, 257-289
 32. Leach, D. L., Taylor, R. D., Fey, D. L., Diehl, S. F., and Saltus, R. W. (2010). A deposit model for Mississippi Valley-Type lead-zinc ores, in: *Mineral deposit models for resource assessment*. USGS Scientific Investigations Report 2010-5070-A, 52pp
 33. Lindsay, J. F., and Martin, D. B. (1999). Stable isotopes – signposts for mineralization, a new regional exploration tool. *Australian Geological Survey Organization research newsletter* 30, 17-19
 34. Marquillas, R., Sabino, I., Sial, A. N., del Papa, C., Ferreira, V., and Matthews, S. (2007). Carbon and Oxygen isotopes of Maastrichtian-Danian shallow marine carbonates: Yacoraite Formation, northwestern Argentina. *Journal of South American Earth Sciences* 23, 304-320
 35. Marshall, J. D. (1992). Climatic and oceanographic signals from the carbonate rock record and their preservation. *Geological Magazine* 129, 143-160
 36. McCrea, J. M. (1950). On the isotope chemistry of carbonates and a paleo-temperature scale. *Journal of Chemistry and Physics* 18, 849-857
 37. Morse, J. W., and MacKenzie, F. T. (1990). *Geochemistry of sedimentary carbonates*. *Developments in Sedimentology* 48, 707pp
 38. Moss, S., and Tucker, M. E. (1995). Diagenesis of Barremian-Aptian platform carbonates (the Urgonian Limestone formation of SE France): Near-surface and shallow burial diagenesis. *Sedimentology* 42, 853-874

39. Nagarajan, R., Sial, A. N., Armstrong Altrin, J. S., Madhavaraju, J., and Nagendra, R. (2008). Carbon and Oxygen isotope geochemistry of Neoproterozoic limestones of Shahabad Formation, Bhima Basin, Karnataka, South India. *Revista Mexica de Ciencias Geologicas* 25, 225-235
40. Peace, M. W., Wallace, M. W., Holdstock, M. P., and Ashton, J. H. (2003). Ore textures within the U lense of the Navan Zn-Pb deposits, Ireland. *Mineralium Deposita* 38, 568-584
41. Prokoph, A., Shields, G. A., and Veizer, J. (2008). Compilation and time-series analysis of a marine carbonate $\delta^{18}\text{O}$, $\delta^{13}\text{C}$, $^{87}\text{Sr}/^{86}\text{Sr}$ and $\delta^{34}\text{S}$ database through earth history. *Earth Science Reviews* 87, 113-133
42. Senbeto Chewaka, and De Wit, M. J. (Eds.) (1981). Plate tectonics and metallogenesis: some guidelines to Ethiopia mineral deposits. Ethiopian Institute of Geological Survey, Bull. 2, pp.1-129
43. Shackleton, N. J., and Kennett, J. P. (1975). Paleotemperature history of the Cenozoic and the initiation of Antarctic glaciation: Oxygen and carbon isotope analyses in DSDP sites 277, 279 and 281. In: Kennett J P, Houtz R E et al. (Eds.), Initial Reports of the Deep Sea Drilling Project 29. US Government Printing Office, Washington, pp.743-755
44. Sial, A. N., Ferreira, V. P., Toselli, A. J., Parada, M. A., Acenolaza, F. G., Pimentel, M. M., and Alonso, R. N. (2001). Carbon and Oxygen isotope composition of some Upper Cretaceous-Paleocene sequences in Argentina and Chile. *International Geological Review* 43, 892-909
45. Spangenberg, J., Fontbote, L., Sharp, Z. D., and Hunziker, J. (1996). Carbon and oxygen isotope study of hydrothermal carbonates in the zinc-lead deposits of the San Vicente district, central Peru: a quantitative modeling on mixing processes and CO_2 degassing. *Chem Geol* 133(1-4), 289-315
46. Stegen, R. J., Beaty, D. W., and Thompson, T. B. (1990). The origin of the Ag-Pb-Zn-Ba deposits at Aspen, Colorado, based on geologic and geochemical studies of the Smuggler orebody: *Economic Geology Monograph* 7, pp.266-300
47. Sverjensky, D. A. (1984). The origin of a Mississippi Valley-type deposit in the Viburnum Trend, Southeast Missouri. *Economic Geology* 76 (7), 1848-1872.
48. Sverjensky, D. A. (1984). Oil field brines as ore-forming solutions. *Economic Geology* 79 (1), 23-37
49. Sverjensky, D. A. (1986). Genesis of Mississippi Valley Type Pb-Zn Deposits. *Annual Review Earth Planetary Science* 14, 177-199
50. Thompson, T. B., and Arehart, G. B. (1990). Geology and the origin of ore deposits in the Leadville district, Colorado: Part II. Oxygen, hydrogen, carbon, sulfur, and lead isotope data and the development of a genetic model. *Economic Geology Monograph* 7, 156-179
51. Tucker, M. E. (1991). The diagenesis of fossils; in Dobovan SK (ed.), *The process of fossilization*, pp.84-104. Belhaven Press, London
52. Tucker, M. E., and Wright, V. P. (1990). *Carbonate Sedimentology*. Blackwell, Oxford
53. Veizer, J. (1983). Chemical Diagenesis of carbonates: theory and application of trace element technique, in: Arthur M A, Anderson T F, Kaplan I R, Veizer J, Land L S (eds.), *Stable isotopes in sedimentary geology*. Soc. Eco. Petrol. Mineral. Short Course 10, Tulsa, 3.1-3.100
54. Vincent, B., Emmanuel, L., Houel, P., and Loreau, J. P. (2007). Geodynamic control on carbonate diagenesis: Petrographic and isotopic investigation of the Upper Jurassic formations of the Paris Basin (France). *Sedimentary Geology* 197, 267-289
55. Worash Getaneh and Valera, R. (2002). Rare earth element geochemistry of the Antalo Supersequence in the Mekele Outlier (Tigray region, Northern Ethiopia). *Chemical Geology* 182(2-4), 395-407